Analysis of Droplet Coalescence in Emulsions Subjected to Acoustic Fields

Gautam D. Pangu and Donald L. Feke, Department of Chemical Engineering,
Case Western Reserve University, Cleveland, OH 44106 USA

Abstract

Separation and recovery of the oil phase from emulsions has practical applications in a variety of situations, including environmental remediation, pharmaceutical manufacture, and food processing. In our laboratory, we have developed methods for such separations by applying a low-intensity, resonant ultrasonic field within a rectangular chamber, which is optionally filled with a highly porous mesh. The density and compressibility difference between the dispersed phase droplets and the continuous phase results in a net force on the droplets. The drops migrate to the pressure antinodes of the standing wave field under the influence of this primary acoustic force. Subsequent coalescence of the droplets takes place due to interdroplet forces. Efficient coalescence and transport of the oil droplets was experimentally demonstrated and oil separation efficiencies as high as 90% were observed in laboratory-scale devices.

The present work focuses on obtaining fundamental understanding of the relevant physical and chemical phenomena that underlie the transport and coalescence of droplets observed in these experiments. A microscopic mathematical model is developed which includes pertinent body forces (buoyancy and the primary acoustic force) and interdroplet effects (van der Waals forces, hydrodynamic interactions and secondary acoustic forces) that govern the phenomena. The model predicts the relative motion of a pair of droplets, given various parameters like the strength and frequency of the sound field, the initial positions of the two interacting drops, their sizes, plus the viscosity and density of both the continuous and dispersed phases. The results from this model are used to compute the collision rate for a given droplet pair in acoustic field. This leads to the development of a macroscopic population balance model to predict the evolution of drop-sizes in a given drop population coalescing under the influence of acoustic field. Such predictions can then be validated by performing experiments to track the droplet size distribution of an emulsion subjected to an acoustic field.

Introduction

The recovery of micron- to millimeter-sized dispersed liquid droplets from a liquid emulsion is of fundamental and practical importance in many chemical, petrochemical, and biological process applications. Conventional methods for liquid-liquid phase-separation approaches involve either physical (e.g., gravity, centrifugal or electrical fields) or chemical (use of additives that alter molecular interactions) approaches. Chemical methods have the disadvantage of cost and the complication of utilizing a chemical that might need to be removed in subsequent steps of the process. Physical methods can be slow, occupy large physical space, or require sophisticated equipment. Difficulties involved in scale-up of these processes and maintaining high efficiencies on a large scale over longer periods of time may pose problems in using these processes for practical applications.

During the past two decades, phase-separation methods based on the use of ultrasonic fields have received increasing attention. Suspended particles or droplets respond to resonant acoustic fields if there is a non-zero acoustic contrast between the dispersed and host phases. Processes utilizing combinations of acoustic forces with hydrodynamic, gravitational or diffusion forces have been experimentally studied and modeled. In several of these methods, a one-dimensional sound field is used to organize the particles into thin parallel bands separated by one-half acoustic wavelength spacing. The particles are separated from their suspending fluid by either positioning closely spaced physical barriers between the bands of particles[1-3] or transporting particles in opposite direction of the flowing fluid by using pseudo-standing waves[4,5]. Some of the acoustic methods intend to induce agglomeration of particles by secondary acoustic forces and the resulting agglomerates are then removed by conventional techniques such as physical screening techniques or gravity driven methods.[6,7]

Certain of these techniques blend acoustic and physical screening methods by applying a resonant acoustic field to a porous mesh through which a particle suspension flows. The interaction of acoustic field with the porous mesh improves its performance as a filter and collection of particles up to two orders of magnitude smaller than the pore size of the mesh can be achieved. Deactivating the acoustic field allows the trapped particles to be flushed from the porous mesh and recovered separately.[8]

In this paper, we focus attention on a process intended to recover the oil phase from aqueous emulsions (droplet size ranging from 1-15 μm). Specifically, a resonant ultrasonic wave-field is applied to the emulsion flowing through a rectangular chamber. The oil droplets respond to the acoustic and other relevant forces and are transported toward eventual coalescence events. Figure 1 presents images that illustrate the phenomena. Shown is the vertical cross-section of an acoustic chamber before and after the activation of the acoustic field. A dilute (~ 0.5 vol%) emulsion of vegetable oil dispersed in water, having a mean droplet diameter of 3 μm is subjected to the acoustic radiation. Prior to the activation of the field, the emulsion appears to be homogenous (Fig. 1a) but very soon after the acoustic field was turned on, comparatively larger droplets become visible inside the chamber (Fig. 1b). These coalesced droplets typically show a strong tendency to migrate towards the internal surfaces of the chamber. When a porous mesh is used inside the chamber, the droplets are retained inside the mesh and the performance of the mesh is observed to depend on its acoustic and wetting properties.[9]

Our work aims at developing a fundamental understanding of the acoustically induced bulk coalescence through a modeling approach. We build this model by first studying the rate of collision between individual pairs of droplets located at prescribed starting positions within an acoustic chamber. Subsequently, we use this pair interaction model to assemble a prediction of the evolution of droplet size distribution with time under different processing conditions. The results can be tested against experimental observations and the model itself can be used as the basis for process design and scale-up.

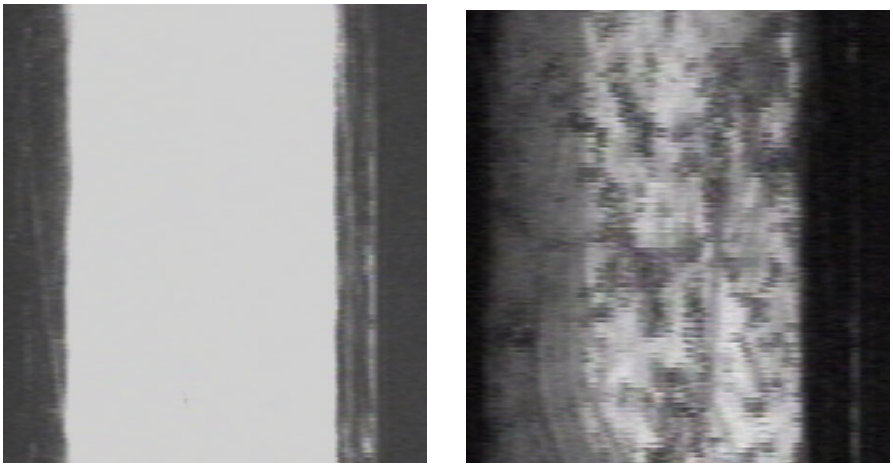

(a) (b)

Figure 1: Photographs of the vertical cross-section of the chamber for the case of no internal porous medium: (a) before activation of the acoustic field; (b) one minute after the acoustic field is activated. The results of droplet coalescence and retention inside the chamber can be seen.

Droplet Pair Model Development

The acoustic force that acts on suspended droplets is sensitive to the physical properties of the system (e.g., droplet size distribution, density and compressibility difference between the droplets and host liquid) and processing parameters (e.g., acoustic intensity and frequency). We consider the consequences of applying a one-dimensional ultrasonic standing-wave field to a dilute emulsion containing spherical drops of viscosity μ' and density ρ' dispersed in an immiscible fluid of viscosity μ and density ρ. Surface tension effects are presumed strong enough to keep the droplets from being distorted from a spherical shape by the combination of forces acting upon them. The system is considered to be isothermal. Both fluids are considered to be Newtonian, and it is assumed that there are no relevant surfactant effects at the drop surface. Droplets are assumed to be small enough that inertial forces can be neglected. The analysis is restricted to dilute emulsions for which only the binary interaction of droplets need be considered, and for the case of Peclet numbers much greater than unity, i.e. when the external forces dominate over Brownian diffusion. It is assumed that every droplet collision results in irreversible coalescence of the droplets, and that coalescence proceeds without delay upon droplet collision. The pair of interacting droplets is assumed to be located within a half-wavelength-wide region between two pressure nodes prior to the application of the acoustic field. The droplet radii are a_1 and a_2 and their location relative to the pressure antinode at time t = 0 are y_1^0 and y_2^0 respectively. The relative position of the two droplets is described by the polar coordinates r and θ. Both the gravitational and primary acoustic fields are assumed to be oriented vertically.

The forces considered in the analysis here include gravity, the primary acoustic force, van der Waals attractive force, hydrodynamic interactions and secondary acoustic force. Standard expressions are used for the gravitational and van der Waals attractive forces. The primary acoustic force is given by:

$$F_{1,ac} = 4\pi a^3 \kappa E_{ac} F \sin(2\kappa y) \qquad [1]$$

This time-averaged force is a result of the density and compressibility difference between the dispersed and the continuous phase and it acts in the direction parallel to the direction of the acoustic field [10]. In Eq. 1, κ is the wave number of the acoustic field, E_{ac} is the average energy density of the acoustic field, y is the distance from the pressure antinode, and F is the acoustic contrast factor that quantifies the density and compressibility difference between the drop and the continuous phase, which is given by

$$F = \frac{\hat{\rho} + (2/3)(\hat{\rho} - 1)}{(1 + 2\Lambda)} - \frac{1}{3\sigma^2 \hat{\rho}} \qquad [2]$$

where $\hat{\rho}$ is the ratio of the droplet density to the continuous phase density and σ is the ratio of the speed of sound in the droplet to that in the continuous phase. For oil droplets dispersed in water, F has a negative value. For this condition, analysis of Eq. 1 reveals that the pressure antinodes of the acoustic field are the stable collection points for the droplets.

The secondary acoustic force between two compressible spherical droplets, which results from the interaction of the sound field scattered from each droplet, is given by

$$F_{2,ac} = \frac{\kappa^2 E_{ac}}{2\pi}\left(1 - \frac{\gamma_{p1}}{\gamma_f}\right)\left(1 - \frac{\gamma_{p2}}{\gamma_f}\right)\frac{V_{p2}V_{p1}}{r^2} \qquad [3]$$

where γ_p is the compressibility of the droplet, γ_f is the compressibility of the fluid, V is the droplet volume and r is the center-to-center distance between the droplets[11]. The secondary acoustic force acts along the line of centers of the two particles and it is an attractive force when both particles are either more or less compressible than the fluid. Note that this force scales directly with the product of droplet volumes and inversely with their distance from each other. Thus, as the two droplets approach each other, this force becomes significantly large in magnitude and it can induce their coalescence.

Under the assumption that the inertial forces are negligible, a drag force develops that is equal to and opposite of the net force acting on the droplets. The expression for the drag force on an isolated liquid droplet is given by the Hadamard-Rybczynski formula:

$$F_d = -4\pi\left(\frac{1 + 3\hat{\mu}/2}{1 + \hat{\mu}}\right)\mu a V^0 \qquad [4]$$

where $\hat{\mu}$ is the ratio of the viscosity of the droplet to that of the surrounding fluid and V^0 is the magnitude of the droplet velocity which can be computed by balancing the drag force on a droplet with gravity and primary acoustic force. The difference of V^0 for the two droplets under consideration yields their far-field relative velocity $V_{12}{}^0$.

The far-field velocity is augmented with the near-field interaction between the droplets, including secondary acoustic forces, van der Waals attractive force and hydrodynamic interactions. Haber, *et al.*[12] and Zinchenko[13] developed exact solutions for the hydrodynamic resistance to the drop collision using the method of bispherical coordinates: the former being the solution for the axisymmetric motion of two drops (drops moving along their line of centers) while the latter applies to the asymmetric motion of drops (drops moving normal to their line of centers). Using this analysis, Zhang and Davis[14]derived far-field and near-field expressions for axisymmetric relative mobility functions L and G, and for asymmetric relative mobility function M, as a function of $\hat{\mu}$, $\hat{a}$ and s. The far-field expression is applicable when the droplets are widely separated (typically $s > 3$) and the near-field expression is valid in the near contact region of the two droplets (typically $s < 2.05$). The relative velocity of a droplet pair interacting

under the influence of an acoustic field can thus be obtained following the development of Batchelor[15] and the relative trajectory of the pair can be computed by numerically solving the resulting first-order ordinary differential equations simultaneously.

Results and Discussion

Relative droplet trajectories

To illustrate our modeling approach, we provide simulation results for a typical case representative of experimental trials. Table 1 lists the parameters used in the simulations reported in this paper. An example relative trajectory is shown in Fig. 2a, while Fig. 2b shows dimensionless separation s (=$2r/(a_1 + a_2)$) as a function of time. For this example, the droplets were assumed to be located at a relative angle of 10° from the horizontal with a dimensionless center-to-center distance of s = 24.97. It should be noted that the oval shaped object in Fig. 2a, represents a circular collision surface but appears non-circular due to the different scales used for the horizontal and vertical axes. The results of the droplet-pair coalescence model show that a typical droplet trajectory consists of two regimes: (a) the "fast" relative motion of two drops due to the combination of the primary acoustic force that pushes them to the pressure antinode and gravitational forces; and, (b) the slow approach to collision due to secondary acoustic and van der Waals effects.

Table 1: Parameters for the simulation results shown in Fig. 2.

Parameter	Value
a_1, size of droplet 1	1.5×10^{-5} m
a_2, size of droplet 2	1.6×10^{-5} m
ρ, density of the continuous phase	1000 kg/m^3
ρ', density of the droplet phase	900 kg/m^3
μ, viscosity of the continuous phase	1×10^{-3} kg/m·s
μ', viscosity of the droplet phase	2×10^{-3} kg/m·s
c, speed of sound through the continuous phase	1490 m/s
c', speed of sound through the droplet phase	1430 m/s
E_{ac}, energy density of the acoustic field	100 J/m^3
κ, wave number of the acoustic field	8490.8 m^{-1}
A, Hamaker constant	5×10^{-21} J
T, absolute temperature	298.15 K
y_1^0, starting position of the drop 1	-(λ/4.01), below the top node
y_2^0, starting position of the drop 1	(λ/4.0), at the bottom node

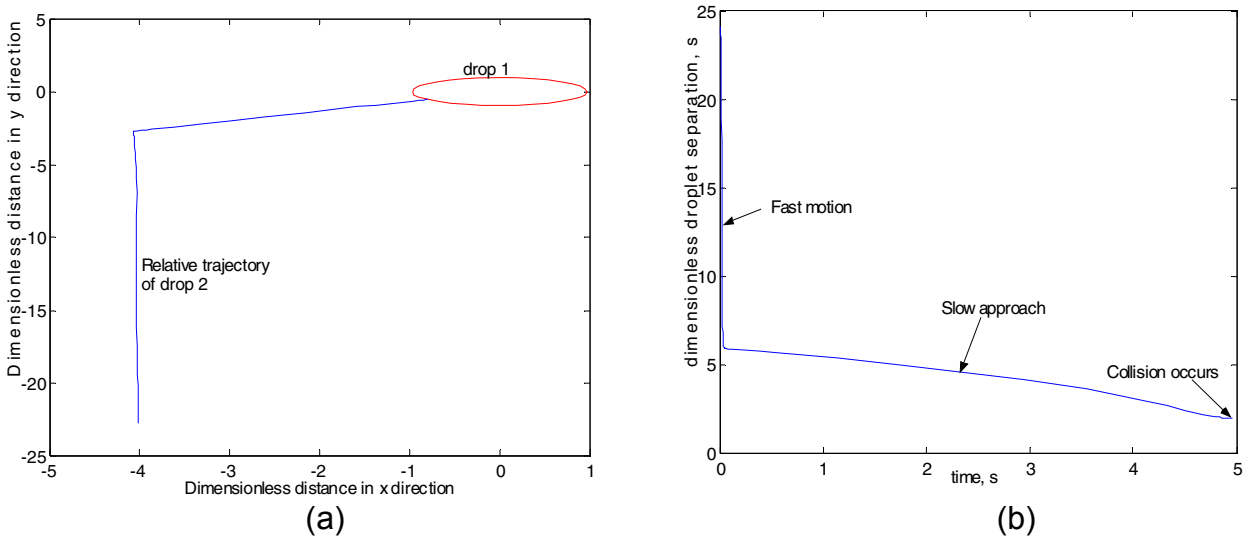

Figure 2: Relative droplet trajectories for the example case: (a) two-dimensional representation of the particle path. (b) relative separation as a function of time.

Iso-time collision contours

While the droplet-pair model serves as a useful tool to understand the basic physical phenomena underlying the relative motion of droplets, it alone is not sufficient to predict overall coalescence rates. Hence, we identify the time to collision as the critical parameter that leads to overall coalescence rates. To analyze and quantify the coalescence phenomena further, the relation between the initial configuration of the droplet pair and the time to collision can be studied. To determine this relation, the initial position of one drop (drop 1), referred to as the reference drop henceforth, was kept constant and the trajectories for a series of incoming droplets with different initial placements were simulated. This procedure was used to map out the region inside of which drop 2 would need to be positioned so that collision with the reference drop occurs within a specified time period. These loci are referred to as "iso-time collision contours."

Fig. 3 shows predicted iso-time contours for a pair of drops having sizes of 9 μm and 18 μm. Since the iso-time contours show cylindrical symmetry (around the *y*-axis), the *x*-coordinate of the initial position of the reference drop is always taken to be zero and the *y*-coordinate of the initial position indicates its distance from the pressure antinode. For the results shown in Fig. 3a, the 18-μm drop was considered as the reference drop and it is located at the antinode at $t = 0$ and the iso-time contours for the 9-μm drop were obtained for $t = 1$, 5, and 10 s. The results for the case where the 18-μm drop was located at the bottom node at $t = 0$ are shown in Fig. 3b. The distances plotted in Fig. 3 in the *x*- and *y*-directions were made dimensionless by using one-quarter wavelength, ($\lambda/4$) as the scale factor. It can be observed from Fig. 3 that the iso-time contours define larger regions for extended coalescence times.

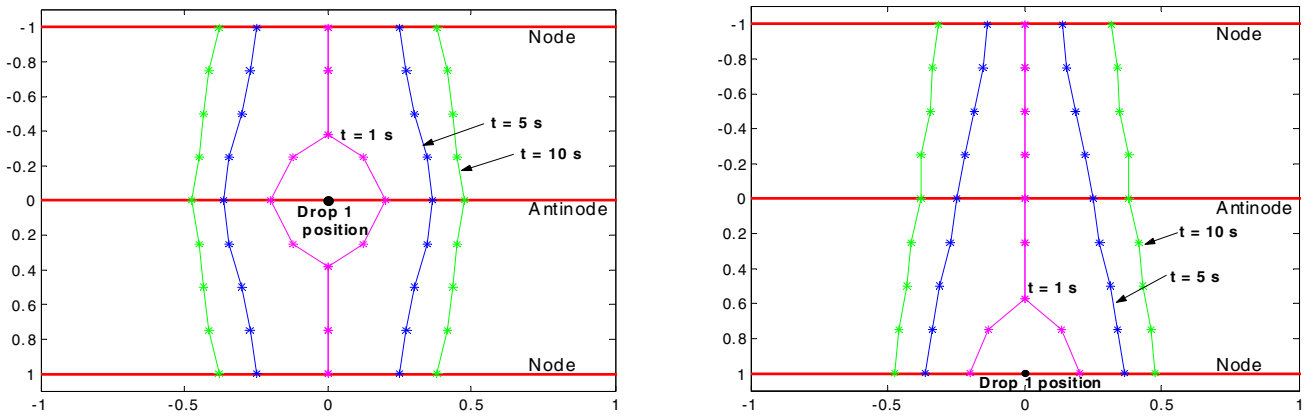

Figure 3: Iso-time contours for the interaction of a 9-μm and 18 μm droplet pair: (a) the 18-μm drop is located at antinode at t = 0; and, (b) the 18-μm drop is located at bottom node at t = 0.

The volume enclosed by an iso-time collision contour will be a function of the relative size of the two drops, the physical properties of the dispersed and host phases, plus the frequency and intensity of the acoustic field. This volume will also be an indication of the coalescence rate of a given droplet pair. Hence it can be used as a parameter that bridges the microscopic droplet-pair model with a global population balance model that aims to predict the size-evolution of a drop population coalescing under the influence of an acoustic field.

Global Model Development

The results of the droplet pair model are applied to predict the droplet size-evolution in a quiescent emulsion inside a chamber under the influence of an acoustic field. All the droplets migrate to the nearest antinodal plane within a few seconds after the acoustic field is activated as long as the magnitude of the primary acoustic force is greater than buoyancy effects, i.e. if

$$\left|\frac{3\kappa E_{ac} F}{(\rho'-\rho)g}\right| > 1 \qquad [5]$$

The location of the droplet collection plane is independent of droplet size. Once a droplet migrates to its collection plane, its velocity due to body forces becomes zero. The resulting simplified relative droplet-pair trajectory equations can be solved to obtain the area cleared by coalescence of a droplet pair as a function of the droplet properties and the acoustic field parameters. These predictions for cleared area are incorporated into standard population balance models for the prediction of the evolution of the droplet size distribution with sonication time.

If a_1 is the radius of the drops in a monodisperse emulsion prior to the application of the acoustic field, the radius of the drop of size-category i is given as $a_i = a_1 i^{1/3}$. If n_i^t is the instantaneous number density of the drops of size a_i, the population balance equation that describes the evolution of n_i^t can be obtained by a mass balance on drops of that size category:

$$\frac{\Delta n_i}{\Delta t} = \frac{\lambda}{2}\left(\frac{1}{2}\sum_{j=1}^{i-1} A_{j,i-j} n_i^t n_{i-j}^t - \sum_{i=1}^{n} A_{i,j} n_i^t n_j^t\right) \quad [6]$$

where $A_{i,j}$ is the area cleared by coalescence of drops of size-categories i and j in time Δt. The first term on the right-hand side of Eq. 6 represents the rate of formation of drops of size-category i by collisions of two smaller drops, the factor of ½ is used to avoid double counting, and the second term represents the rate of consumption of drops of size-category i due to their collisions with other drops. Thus the number of drops of size-category i at time $(t + \Delta t)$ would be given by

$$n_i^{t+\Delta t} = n_i^t + \Delta n_i \quad [7]$$

Starting with a given initial size-distribution of the emulsion prior to the application of acoustic field, Eqs. 6 and 7 are solved at each time step to compute the change in number density of drops of each size-category during that time interval. After every time step, the new droplet size distribution is determined after taking into account the number density of newly formed larger drops and Eqs. 6 and 7 are again solved to track the size-evolution of given droplet population. Fig. 4a shows one such prediction for the case of an initially monodisperse 0.5 vol% emulsion subjected to a typical ultrasonic field. Fig. 4b shows the size distribution predicted following 5 min of sonication for two different acoustic field strengths. As expected, the stronger the acoustic field, the coarser the emulsion that is predicted at fixed sonication times.

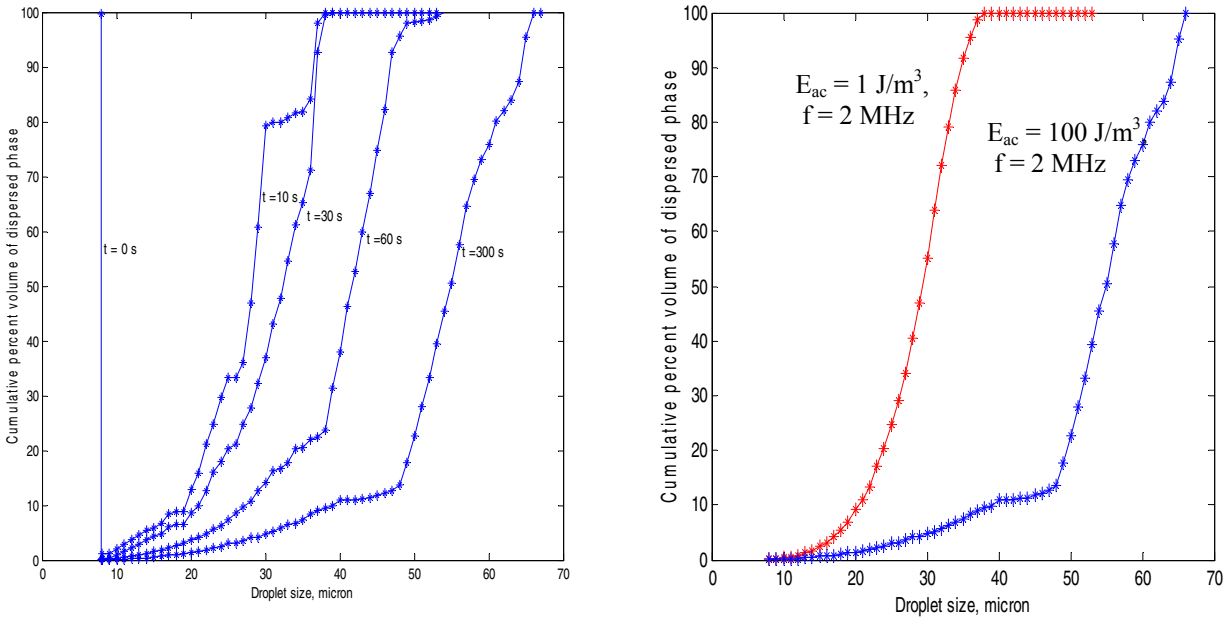

Fig. 4: (a) Prediction of droplet size distribution as a function of sonication time for the case of an initially monodisperse emulsion (radius = 8 μm), E_{ac} = 100 J/m^3, and f = 2 MHz. (b) Prediction of the effect of acoustic field strength on the droplet size distribution after 5 min of sonication.

Validation of Global Model

The coalescence predictions of the global model were validated by tracking the size-evolution of an emulsion under the influence of an acoustic field experimentally. A chamber filled with an emulsion was placed in the sensing zone within a laser particle counter and the acoustic field was activated. The droplet size distribution of the emulsion was measured while coalescence occurs within the acoustic field. To obtain an estimate of the acoustic energy density E_{ac} within the liquid under experimental conditions, a chamber optimization model[16] that predicts the E_{ac} distribution in various layers of the acoustic chamber, given their mechanical properties and dimensions, was used. This E_{ac} value was used for the global model computations to obtain the predictions of droplet size-evolution in an emulsion with the same initial size distribution as that of the experimental emulsion.

A comparison of model predictions and experimental observations for the size-evolution in an emulsion reveals that the model predictions agree qualitatively with the experimental results, and they also match the experimentally observed trends in size-evolution with change in E_{ac} and frequency. However the results indicate that the model consistently under-predicts the rate of coalescence in an emulsion. Fig. 5 shows a typical comparison of model predictions with experimental results. The degree of coalescence as observed experimentally is always more than that predicted by the model.

In the development of droplet pair model and global model, the effects of a one-dimensional sound field on droplet transport and coalescence are considered. However for a variety of reasons, the sound field inside the acoustic chamber can acquire a three-dimensional character to a certain degree which could lead to gradients in E_{ac} within the chamber. For a standing wave-field with non-uniform amplitude in directions perpendicular to its propagation, in addition to primary axial acoustic radiation force given by Eq. 1, a lateral

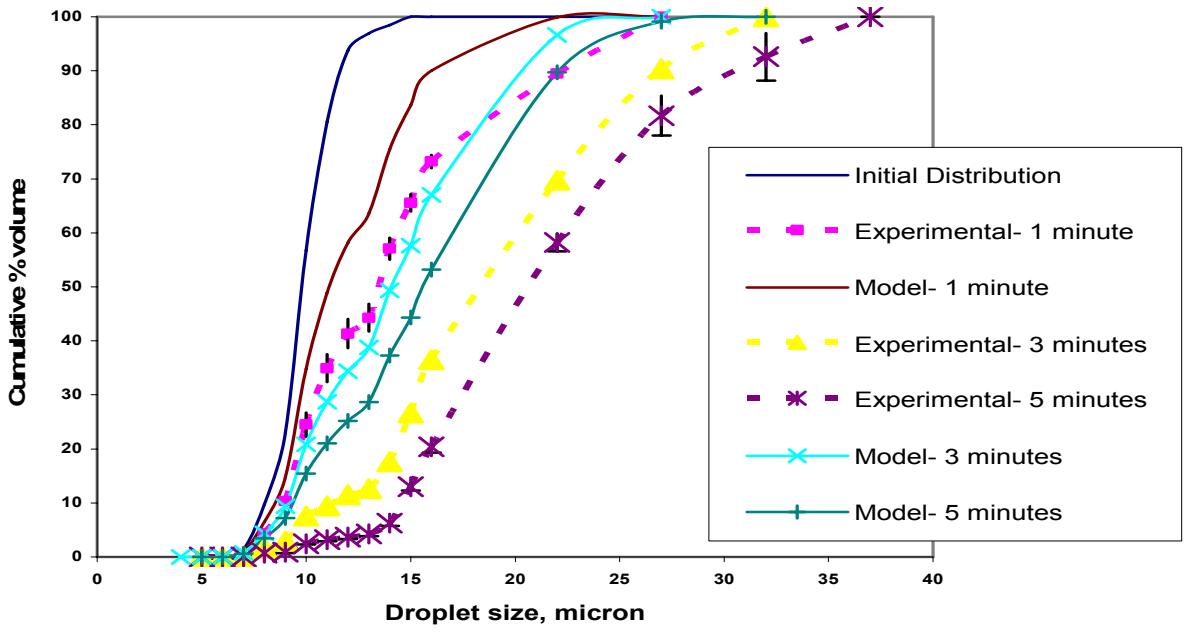

Fig. 5: Comparison of experimental results and model predictions of coalescence in an emulsion for E_{ac} = 56 J/m^3 and f = 1.69 MHz.

component of acoustic radiation force also acts on the particles. This force scales directly with the gradients of E_{ac}, and hence it is typically at least an order of magnitude smaller than the axial primary acoustic force. However once the axial force causes particle migration to the antinodal planes, the lateral force can cause them to aggregate at the local E_{ac} maxima[17]. This effect could have caused the droplets to concentrate in the regions of local E_{ac} maxima within an antinodal plane, which in turn would lead to an increased rate of coalescence.

To incorporate lateral radiation forces in the model, the three-dimensional distribution of E_{ac} within the liquid could be measured experimentally. To obtain a gauge of the contribution of these lateral forces to overall coalescence, the experimental results were compared with the model predictions (without incorporating the lateral forces) and an effective E_{ac} value at which both results match well were obtained. Typically these effective E_{ac} values were found to be 2-3 times greater than the E_{ac} predicted by the chamber optimization model. E_{ac} variations of this scale have been observed by other researchers in their experimental devices[18], and hence these effective E_{ac} values can be used to obtain predictions of coalescence in an emulsion using the currently developed droplet pair model and global coalescence model.

Conclusions

The transport and coalescence of micron-scale emulsions through the application of acoustic fields has been demonstrated in laboratory experiments. In order to provide a theoretical basis for the observed phenomena and to enable modeling of the process for design and scale-up purposes, a trajectory model for the relative motion of pairs of droplets has been developed. This analysis incorporates the fundamental primary (acoustic, gravity, buoyancy, and hydrodynamic) and secondary (acoustic, van der Waals) forces that act to determine the relative motion of the droplets.

In order to quantify the prediction of coalescence rates, we introduce the concept of iso-time collision contours, which are the loci of the regions of initial positions of the droplets that lead to a collision within a specified time. Assessment of the size of these regions as a function of sonication conditions and then performing spatial averaging enables prediction of the overall rates of pair coalescence. These results are further used in a standard population balance approach to predict the evolution of the droplet size distribution within an emulsion subjected to sonication.

The results of the population balance model have been experimentally validated and a good agreement has been found between model predictions and experimental results. The model can be further strengthened by incorporating the contribution of lateral acoustic forces to the coalescence phenomena.

Acknowledgment

The authors are grateful to Nestle R&D for financial support of this work.

References

1. Z.I. Mandralis, D. L. Feke, *A.I.Ch.E. Journal* **39,** 197 (1993).
2. Z. I. Mandralis, D. L. Feke, *Chem. Eng. Sci*. **48,** 3897 (1993).
3. S. Gupta, D. L. Feke, I. Manaz-Zloczower, *Chem. Eng. Sci.* **50,** 3275 (1995).
4. T. L. Tolt, D. L. Feke, *J. Acoust. Soc. Am*. **91,** 3152 (1992).
5. E. Benes, F. Hager, W. Bolek, M. Groschl, Ultrasonics International 93 Conference Proceedings, Butterworth-Heinemann, Oxford, UK, 167.
6. A. Frank, W. Bolek, M. Groschl, W. Burger, E. Benes, Ultrasonics International 91 Conference Proceedings, Butterworth-Heinemann, Oxford, UK, 519.
7. R. Allman, W. T. Coakley, *Bioseparation* **4,** 29 (1994).
8. S. Gupta, D. L. Feke, *A.I.Ch.E. Journal* **44,** 1005 (1998).
9. G. D. Pangu, D. L. Feke, *Chem. Eng. Sci.* **59**, 3183 (2004).
10. K. Yosioka, G. Kawasima, *Acustica* **5,** 167 (1955).
11. M. A. H. Weiser, R. E. Apfel, *Acustica* **56,** 114 (1984).
12. S. Haber, G. Hetsroni, A. Solan, *Int. J. Multiphase Flow* **4,** 1 (1978).
13. A. Z. Zinchenko, *J. Appl. Math. Mech.* **44,** 30 (1980).
14. X. Zhang and R. H. Davis, *J. Fluid Mech.* **230**, 479 (1991).
15. G. K. Batchelor, *J. Fluid Mech.* **119,** 379 (1982).
16. D. Rusinko, *Design and optimization of an ultrasonic standing wave chamber*, M.S. Thesis, Case Western Reserve University, Cleveland, OH (2001).
17. G. Whitworth, W. T. Coakley, *J. Acoust. Soc. Am.* **91**, 79 (1992).
18. S. M. Woodside, M. Groeschl, E. Benes, B. D. Bowen, J. M. Piret, American Chemical Society, San Francisco, CA, ACS, Washington DC.